



King's Research Portal

DOI:

[10.1088/2053-1583/ab9a0f](https://doi.org/10.1088/2053-1583/ab9a0f)

[Link to publication record in King's Research Portal](#)

Citation for published version (APA):

Costa, P. M., Mei, K.-C., Kreuzer, M., Li, Y., Neveen, H. A., Grant, V., Festy, F., Pollard, S. M., & Al-Jamal, K. T. (2020). Selective toxicity of functionalised graphene oxide to patients-derived glioblastoma stem cells and minimal toxicity to non-cancerous brain tissue cells. *Materials*, 7(4), Article 045002. <https://doi.org/10.1088/2053-1583/ab9a0f>

Citing this paper

Please note that where the full-text provided on King's Research Portal is the Author Accepted Manuscript or Post-Print version this may differ from the final Published version. If citing, it is advised that you check and use the publisher's definitive version for pagination, volume/issue, and date of publication details. And where the final published version is provided on the Research Portal, if citing you are again advised to check the publisher's website for any subsequent corrections.

General rights

Copyright and moral rights for the publications made accessible in the Research Portal are retained by the authors and/or other copyright owners and it is a condition of accessing publications that users recognize and abide by the legal requirements associated with these rights.

- Users may download and print one copy of any publication from the Research Portal for the purpose of private study or research.
- You may not further distribute the material or use it for any profit-making activity or commercial gain
- You may freely distribute the URL identifying the publication in the Research Portal

Take down policy

If you believe that this document breaches copyright please contact librarypure@kcl.ac.uk providing details, and we will remove access to the work immediately and investigate your claim.

PAPER

Selective toxicity of functionalised graphene oxide to patients-derived glioblastoma stem cells and minimal toxicity to non-cancerous brain tissue cells

To cite this article: Pedro M Costa *et al* 2020 *2D Mater.* 7 045002

View the [article online](#) for updates and enhancements.



PAPER

OPEN ACCESS







RECEIVED
2 November 2019REVISED
1 June 2020ACCEPTED FOR PUBLICATION
5 June 2020PUBLISHED
9 July 2020

Original content from this work may be used under the terms of the [Creative Commons Attribution 4.0 licence](#).

Any further distribution of this work must maintain attribution to the author(s) and the title of the work, journal citation and DOI.



Selective toxicity of functionalised graphene oxide to patients-derived glioblastoma stem cells and minimal toxicity to non-cancerous brain tissue cells

Pedro M Costa^{1,6} , Kuo-Ching Mei^{1,6} , Martin Kreuzer² , Yueting Li^{1,3}, Hosny A Neveen⁴, Vivien Grant⁵, Frederic Festy⁴ , Steven M Pollard⁵  and Khuloud T Al-Jamal¹ 

¹ School of Cancer & Pharmaceutical Sciences, Faculty of Life Sciences & Medicine, King's College London, Franklin-Wilkins Building, London SE1 9NH, United Kingdom

² ALBA Synchrotron Light Source, Carrer de La Llum 2-26, Barcelona, Cerdanyola del Valles 08290, Spain

³ Key Laboratory of Pharmaceutics of Guizhou Province, Guizhou Medical University, No. 9, Beijing Road, Yunyan District, Guiyang 550004, People's Republic of China

⁴ Tissue Engineering and Biophotonics, Dental Institute, King's College London, Guy's Hospital Campus, London SE1 9RT, United Kingdom

⁵ MRC Centre for Regenerative Medicine, University of Edinburgh, Edinburgh bioQuarter, 5 Little France Drive, Edinburgh EH16 4UU, United Kingdom

⁶ Contributed equally to this work

E-mail: khuloud.al-jamal@kcl.ac.uk and steven.pollard@ed.ac.uk

Keywords: Brain, glioblastoma (GBM), glioblastoma stem-like cells (GSCs), graphene oxide, click chemistry, cell toxicity

Supplementary material for this article is available [online](#)

Abstract

Glioblastoma (GBMs) is an aggressive type of brain tumour, driven by immature neural stem cell-like cells that promote tumour growth and underlie resistance to conventional therapy. The GBM stem cells (GSCs) can exist in quiescent or dormant states and infiltrate widely into surrounding brain tissues, currently incurable with only around one-year median survival. Innovative therapeutic strategies for GBMs are urgently needed. Here we explore functionalized graphene oxide (GO) to assess their value as delivery vehicles for GBM therapeutics. Interactions and cellular responses were assessed *in vitro* using both classic cell lines and patient derived GSCs. Association between the functionalised GO and established GBM cell lines (serum grown 'non-stem' cells) was strong and resulted in decreased cell viability, increased cell oxidative stress, and changes in lipids composition in a concentration-dependent manner. Responses were more moderate in GSCs and were only observed at highest functionalised GO concentrations. However, no significant toxicity was detected in brain astrocytes and endothelial cells. These results indicate selective toxicity to highly proliferative GBM cell lines and patient GSCs, with minimal toxicity to normal neural cells and brain tissue. We conclude that a novel class of GBM-targeting graphene-based nanocarriers could be useful delivery vehicles for GBM therapeutics.

1. Introduction

Glioblastoma (GBM) is the most common and lethal type of primary brain tumour. GBM tumours invariably regrow after surgical resection, chemo- and radiotherapy. The median survival after standard treatments is around one year [1]. Accumulating evidence shows that recurrence of this type of tumour is driven by a subset of quiescent GBM stem cells, which share phenotypic and molecular programs with normal neural stem cells and resistant to therapy. These cells can self-renew, proliferate and

differentiate (albeit corrupted and inefficient) [2, 3]. GSCs were also shown to form tumours in animals upon xenotransplantation [3]. However, understanding the critical molecular and cellular alterations that underpin therapy resistance has yet to translate into improved clinical outcomes. To seek for more efficient treatments, GSCs can be expanded *in vitro* using NSC culture conditions while retaining tumour-initiating potential and disease-relevant genetic and epigenetic profiles, which serve as *in vitro* tractable cellular models for the testing of new therapeutics [4–6].

Over the last decade, graphene-based composites formed of a single layer of carbon atoms, have attracted significant interest in biomedicine, due to their exceptional physicochemical properties [7]. Since graphene has very low dispersibility in water, various surface modification strategies, a.k.a. functionalization, have been explored to improve biocompatibility for biomedical applications, e.g. nanoscale drug delivery systems for small molecular and siRNA [8–10], radio-frequency therapy [11] and simultaneous therapy, sensing and bio-imaging purposes [12]. One of the popular ways to functionalize nanomaterials for drug delivery is via biorthogonal chemistry, e.g. copper(i) catalysed azide-alkyne cycloaddition (a.k.a. CuAAC or click chemistry) [13]. Alkyne-functionalized graphene oxide (GO) has been used in different biological applications, from photo-activation to drug delivery. Double functionalised GO containing both azide and protected alkyne (Click² GO) has also been pioneered by our group and was exploited for drug delivery and biomedical applications [14–18]. Here we explore the potential use of Click² GO as GSCs targeting nanotherapeutics by studying the bio-nano interactions and cellular responses of cultured non-proliferating brain-derived cells (e.g. brain endothelial cells and astrocytes), patient-derived GSCs, and a classic non-stem GBM cancer cell line (which display astrocytic features, but not neural stem cell identity).

2. Materials and methods

2.1. Cell culture

Dulbecco's Modified Eagle's Medium (DMEM) low glucose and high glucose, DMEM/Ham's F12 nutrient mixture, dimethyl sulfoxide, MEM non-essential aminoacids (NEAA), D-Glucose solution, laminin, accutase and the superoxide dismutase (SOD) determination kit were acquired from Sigma-Aldrich (UK). Growth factors EGF and FGF-2 were acquired from Peprotech (UK), and the CytoTox 96[®] Non-Radioactive Cytotoxicity Assay was obtained from Promega (UK). Advanced RPMI 1640, penicillin-streptomycin 100X, GlutaMAX[™], phosphate buffered saline (PBS) 10X, BSA fraction V solution 7.5%, β -mercaptoethanol, B-27[®], N-2[®], propidium iodide, and the CellTrace[™] Far Red Cell Proliferation kit were acquired from ThermoFisher Scientific (UK). A complete list of chemicals used on the synthesis/functionalization of GO, and the isolation and purification of primary porcine brain endothelial cells (PBEC) and rat astrocytes in Supplementary Material.

2.2. Synthesis of graphene oxide (GO) and Click² GO

The detailed procedure for the synthesis of GO and Click² GO is provided in supporting material. To reduce the sheet size, Click² GO was sonicated for

6 h on an ice water bath. Ice water was replaced every 30 min to keep the temperature low. Click² GO water dispersions ($3 \text{ mg ml}^{-1} \times 30 \text{ ml}$ per 50 ml tube) were bath sonicated for 10 min then frozen in liquid nitrogen (with gentle shaking during freezing). Samples were placed $\sim 5 \text{ cm}$ above the condense chamber in a Lyotrap freeze dryer (LTE Scientific Ltd., UK. SN: J5467/5) at $-55 \text{ }^\circ\text{C}$ under vacuum at $<0.05 \text{ mbar}$ (RV3 oil sealed rotary vane pump, Edwards, UK) to freeze dry. The final product was a highly porous, black spongy Click² GO cake.

2.3. Attenuated total reflectance Fourier transform infrared (ATR-FTIR) of the nanomaterials

ATR-FTIR analysis was performed in freeze-dried Click² GO using the PerkinElmer[®] Frontier[™] FT-IR equipped with ATR accessory (diamond ATR polarization accessory with 1 reflection top-plate and pressure arm). Samples were loaded onto the reflection top-plate (enough to cover the entire diamond surface), the pressure arm was set for force gauge between $100 \sim 120$ units, and 15 scans were performed for each sample.

2.4. Raman spectroscopy

For Raman spectroscopy analysis, aqueous dispersions of Click² GO were placed on a calcium fluoride (CaF_2) slide (Crystran Ltd, UK) and air-dried in a fume hood. Measurements were performed using a Renishaw[®] inVia-Reflex spectrometer (UK) with an excitation wavelength of 785 nm, 0.1%–5% laser power and spectral window of 500 cm^{-1} to 3200 cm^{-1} for each sample ($n = 3$). Data were acquired and analysed using Renishaw's WiRE 4.0 software.

2.5. Cell lines and culturing conditions

Bioware[®] brite cell line GL261 red-fluc (GL261-Luc mouse glioma cell line, obtained from Perkin-Elmer (UK), was maintained in Advanced RPMI 1640 supplemented with 10% (v/v) heat-inactivated new-born calf serum, 100 U ml^{-1} penicillin, $100 \text{ } \mu\text{g ml}^{-1}$ streptomycin and 2 mM GlutaMAX[™]. The generation and characterization of Human GSC cell lines G7 (proneural/classical subtype of GBM) G26 (a neural/mesenchymal subtype of GBM) [19–21] from independent patient tumours, as well as the culturing conditions, have been described previously [4, 21, 22]. Briefly, GSCs were cultured using serum-free complete media (DMEM/F12, 1.45 g l^{-1} D-Glucose, 1% NEAA, 1% penicillin/streptomycin, 0.012% BSA fraction V and 0.1 mM β -mercaptoethanol) supplemented with B27 and N2 ($1\times$). Growth factors EGF and FGF-2 (10 ng ml^{-1}) and laminin ($1 \text{ } \mu\text{g ml}^{-1}$), were added freshly before cell split. GSCs were routinely grown to confluence and split typically twice per week after dissociation with Accutase[®] cell detachment solution and centrifugation. All cells were maintained at $37 \text{ }^\circ\text{C}$ under

a humidified atmosphere containing 5% CO₂ and regularly tested for mycoplasma contamination.

2.6. Isolation of primary cells and culturing conditions

The isolation and culturing of porcine brain endothelial cells (PBECs) and rat astrocytes [23, 24] is provided in detail in supporting material.

2.7. Cytotoxicity assessment using the modified lactate dehydrogenase (LDH) assay

GL261-luc (10 000 cells well⁻¹), G7 (10 000 cells well⁻¹), G26 (10 000 cells well⁻¹), PBEC (10 000 cells well⁻¹) and rat astrocytes (10 000 cells well⁻¹) were seeded onto 96-well plates and allowed to set for 24 h. Click2 GO (1 mg ml⁻¹ in DI H₂O) was briefly sonicated before addition to the wells at a final concentration of 10, 50 or 100 μg ml⁻¹. DMSO (10% in cell culture media) was used as positive control for the assay, as it causes cytotoxicity by interfering with membrane permeability. Light microscopy images were captured during cell incubation (10X optical followed by 4X electronic amplification). After 24 or 72 h, cells were washed two to three times with PBS and lysed upon incubation for 1 h at 37 °C with fresh phenol-free DMEM containing 0.9% Triton X-100 (v/v). The cell lysates were subsequently centrifuged for 2 h at 4000 rpm (Eppendorf 5810 R), the supernatant was carefully recovered (to avoid the precipitated cells and Click2 GO) and the activity of LDH was measured CytoTox 96® cytotoxicity assay, following the manufacturer's instructions. Absorbance at 490 nm was measured in a FLUOstar Omega microplate reader (BMG Labtech, Germany). Cell viability was calculated as the percentage of control untreated cells using the following equation:

$$\{(A_{490} \text{ of treated cells} - A_{490} \text{ of negative control}) / (A_{490} \text{ of untreated cells} - A_{490} \text{ of negative control})\} \times 100.$$

Negative control: phenol-free DMEM containing 0.9% Triton X-100.

2.8. Evaluation of cell proliferation by flow cytometry

GL261-luc (60 000 cells well⁻¹), G7 (55 000 cells well⁻¹) and G26 (55 000 cells well⁻¹) cells were seeded onto 12-well plates and allowed to set for 24 h. After dilution the CellTrace™ stock solution in HBSS (to a final concentration of 0.5 μM), the probe was incubated with the cells for 20 min at 37 °C. The cells then washed twice with fresh culture medium, and Click2 GO (1 mg ml⁻¹ in DI H₂O, briefly sonicated) was added to the cells in fresh culture medium at a final concentration of 10, 50 or 100 μg ml⁻¹. At 24 or 72 h of incubation, the cells were detached, washed, resuspended in 400 μl of cold PBS and immediately analyzed in a FACSCalibur flow cytometer (BD Biosciences). CellTrace Far Red fluorescence was evaluated in the FL-4 channel, and a total of 20 000

events were collected. The data were analyzed by Cell Quest software (BD Biosciences).

2.9. Quantification of graphene in cultured cells using Raman spectroscopy

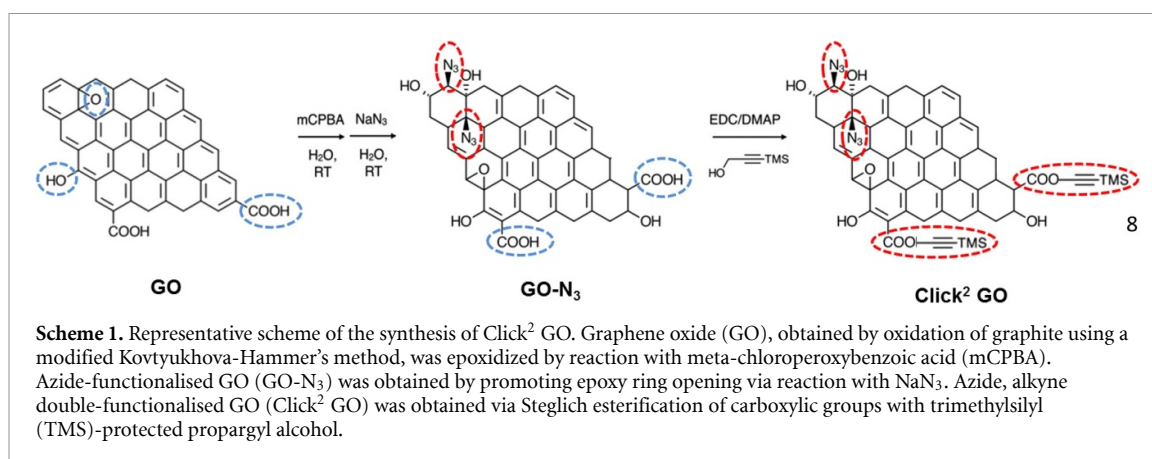
For Raman spectroscopy studies of Click² GO in cultured cells, GL261-luc (70 000 cells well⁻¹), G7 (70 000 cells well⁻¹) and G26 (70 000 cells well⁻¹) cells were seeded on circular CaF₂ coverslips (22 × 0.5 mm) in 6-well plates and allowed to settle for 24 h. The next day, Click² GO (1 mg ml⁻¹ in DI H₂O, briefly sonicated) was added to the cells at a final concentration of 10 or 50 μg ml⁻¹. After 48 h, cells (excluding floating cells) were washed twice with ice-cold PBS and fixed with paraformaldehyde (PFA, 4% in DI H₂O) overnight at 4 °C. The cells were subsequently washed twice with DI H₂O, to remove traces of PFA or PBS that could interfere with measurement and allowed to dry at RT. Raman spectroscopy measurements were performed using an inVia™ Raman microscope (Renishaw, UK) as described in supporting material.

2.10. Oxidative stress analysis using the Superoxide Dismutase (SOD) assay

For oxidative stress measurements, GL261-luc (10 000 cells well⁻¹), G7 (10 000 cells well⁻¹), and G26 (10 000 cells well⁻¹) cells were seeded onto 12-well plates and allowed to settle for 24 h. Cells were then incubated for 24 or 72 h with Click² GO (10, 50 or 100 μg ml⁻¹; 1 ml total volume) or H₂O₂ (2.43 mM). Subsequently, the cells were rinsed 1X with ice-cold PBS, detached using 0.05% Trypsin-EDTA (for 3 min) and, after media inactivation, transferred into 2 ml vials for centrifugation at 4000 rpm (Beckman Coulter Allegra X-22 R) for 10 min at 4 °C. The resulting pellets were washed 2X with ice-cold PBS, resuspended in 200 μl cold PBS followed by two freeze-thawing cycles (freezing in liquid nitrogen, thawing at 37 °C in a water bath) to obtain cell lysates. The lysates were centrifuged at 15 000 × g for 15 min at 4 °C and supernatants were collected to detect the SOD activity (using the SOD determination kit). Briefly, 20 μl of supernatant (or DI H₂O for control samples) was mixed with 200 μl of WST working solution (WS) in a plate, followed by addition of 20 μl of dilution buffer and 20 μl of enzyme working solution (ES). The plate was then incubated at 37 °C for 20 min, and the absorbance was measured at 450 nm (UV/Vis Absorbance Spectra) in a FLUOstar Omega microplate reader (BMG Labtech, Germany) using the Omega 2.10 software. The SOD activity was calculated using the following equation:

$$\text{SOD activity} = \{[(A_{\text{blank 1}} - A_{\text{blank 3}}) - (A_{\text{sample}} - A_{\text{blank 2}})] / (A_{\text{blank 1}} - A_{\text{blank 3}})\} \times 100.$$

Blank 1: 20 μl DI H₂O + 200 μl WS + 20 μl ES; blank 2: 200 μl WS; blank 3: 20 μl DI H₂O + 200 μl WS.



2.11. Synchrotron radiation-based Fourier transform infrared microspectroscopy (SR-FTIR) studies

For SR-FTIR measurements in cultured cells and subsequent PCA analysis, GL261-luc (70 000 cells well⁻¹), G7 (70 000 cells well⁻¹) and G26 (70 000 cells well⁻¹) cells were seeded in CaF₂ coverslips (22 × 0.5 mm) and allowed to settle for 24 h. The next day, Click² GO (1 mg ml⁻¹ in DI H₂O, briefly sonicated) was added to the cells at a final concentration of 10 or 50 μg ml⁻¹. After 48 h, cells (excluding floating cells) were washed 2X with ice-cold PBS and fixed with PFA (4% in DI H₂O) overnight at 4 °C. The cells were subsequently washed 2X with DI H₂O, to remove any traces of PFA and PBS that could interfere with the measurement, and allowed to dry at RT. SR-FTIR was performed at the MIRAS infrared beamline of the ALBA synchrotron (Spain), as described in Supplementary Material.

2.12. Statistical analysis and others

Data are presented as mean ± standard deviation (SD) of at least three different experiments unless otherwise stated. One-way ANOVA combined with the Tukey post-hoc test, was used for multiple comparisons (unless stated otherwise) and considered significant when $p < 0.05$. Statistical differences are presented at probability levels of $p < 0.05$, 0.01 and 0.001. Calculations were performed with Prism 5 (GraphPad, San Diego, CA, USA). Detailed information on GO size measurement by atomic force microscopy, primary porcine brain endothelial cells (PBEC) and rat astrocytes isolation can be found in supporting material.

3. Results

3.1. Production and characterization of graphene oxide derivatives

The synthesis of GO via Mei's modified Kovtyukhova-Hammer's method and surface modification methods to produce Click² GO (Scheme 1) has been previously described in detail [14–16]. Major steps in the GO synthesis include pre-oxidation

of graphite, low-, medium- and high-temperature treatment stages followed by washing and purification, yielding a water-dispersible GO suspension at a concentration of 6.84 mg ml⁻¹, determined by thermogravimetric analysis. GO epoxidation via reaction with meta-chloroperoxybenzoic acid (mCPBA) was performed before reaction with sodium azide to increase epoxy content. Alkyne groups were introduced via Steglich esterification using trimethylsilyl (TMS)-protected propargyl alcohol, to obtain azide and alkyne double functionalised GO (Click² GO) (Scheme 1).

Detailed characterization of the synthesized GO and Click² GO were reported in a recent publication from our group [16]. Briefly, the average surface area of the GO and Click² GO, measured by AFM and TEM, were 186 nm² and 62 nm² before and after sonication, respectively. [16] A 6 h sonication further reduced the medium surface area from 62 nm² to 50 nm² (figures 1(a), (b)). Raman spectroscopy confirmed the presence of the main graphene peaks with the G peak (1597–1600 cm⁻¹) created by stretching of sp² atoms in rings and chains, and the D peak (1316–1325 cm⁻¹) created by stretching of sp² atoms in surface defects. The I_D/I_G ratio, which indicates the degree of surface defects on the graphene flakes, increased after sonication (1.28 ± 0.04 pre-sonication to 1.36 ± 0.12 post-sonication, $p = 0.132$). A shift in the D peak was also detected for sonicated Click² GO, compared to the non-sonicated material ($p = 0.059$) (figure 1(c)).

Infrared (IR) spectroscopy confirmed the introduction of azide groups (peak at 2118 cm⁻¹) and the presence of enhanced C-OH peaks in Click² GO. The alkyne peak could not be detected at 2100–2260 cm⁻¹ as the C ≡ C stretching vibration has weak IR transmittance which overlaps with the azide peak as previously reported (figure 1(d)) [25]. In addition, as shown in our recent publication, the dual-click modification significantly reduced the serum protein binding, i.e. hard protein corona (HC), from 1.44 mg to 0.80 mg HC per mg of GO, a 44% reduction compared to GO. The reduction of HC formation has

linearly correlated with the increase in cellular uptake in phagocytic cells ($r^2 = 0.99634$), *i.e.* Click² GO was taken up ~40%–50% more efficiently than GO at the same time frame [14].

3.2. Double functionalised graphene oxide compromises the viability of glioblastoma cells

The biocompatibility and cellular/molecular interactions and mechanisms of Click² GO on one GBM cell lines GL261 (serum grew), two GSCs G7 and G26 (neural stem cell media), non-dividing primary rat astrocytes, and porcine brain endothelial cells (PBEC) were investigated. Light microscopy images showed an association of Click² GO with all cell types (figure S1 (<https://stacks.iop.org/2DM/7/045002/mmedia>)) at various level after 72 h incubation in the following order: rat astrocytes >GSCs >GL261 >PBEC.

3.2.1. GBM stem-like cells (GSCs)

Phenotypically-distinct tumor-derived human GSCs (G26, G7), previously characterized and tested in stem cell behavior and drug screening studies, were used in these experiments [19, 21]. These cells are maintained as an adherent monolayer culture to provide a more uniform environment that suppresses spontaneous differentiation and to enable direct visualization of cells at single cell resolution [4, 5, 19, 21]. Assessment of cell viability, using a modified LDH assay [26], revealed time-, dose- and GSC type-dependent toxicity of Click² GO (figure 2 and S2) or the parent GO (figure S3): G26 cells were sensitive to Click²GO or GO when incubated at 50 or 100 $\mu\text{g ml}^{-1}$ for 72 h, while toxicity towards G7 cells was only found after incubation with 100 $\mu\text{g ml}^{-1}$ Click² GO for 72 h (~67% cell viability, $p < 0.01$).

3.2.2. Non-stem brain cancer cells

The GL261 murine glioma cell line is widely used in GBM studies as it enables transplantation into immunocompetent animals. For GL216 cells significant toxicity (*i.e.* decreased cell viability) ~ <50% was found for Click² GO at 50 or 100 $\mu\text{g ml}^{-1}$ (24 h) and 10, 50 or 100 $\mu\text{g ml}^{-1}$ (72 h) (figures 2 and S2), as well as for the parent GO at 10, 50 or 100 $\mu\text{g ml}^{-1}$ (72 h) (figure S3).

3.2.3. Non-proliferating brain-derived cells

Having shown that the toxicity of Click² GO in GL261 cells > G26 > G7, experiments were performed to evaluate its toxicity towards non-proliferating brain-derived cells using an *in vitro* blood-brain barrier co-culture model: endothelial cells (which form the brain vascular structure) and astrocytes (provide structural and metabolic support). PBEC cells tolerated well Click² GO (figures 2 and S2) or the parent GO (figure S3) when incubated for 24 h or 72 h at 10, 50 or 100 $\mu\text{g ml}^{-1}$ (>80% cell viability). Average values of >90% cell viability were also obtained following

incubation of astrocytes for 24 or 72 h with Click² GO (figures 2 and S2) or the parent GO (figure S3).

3.3. Double functionalised GO induces oxidative stress reversibly and irreversibly in human GSCs and GL261, respectively

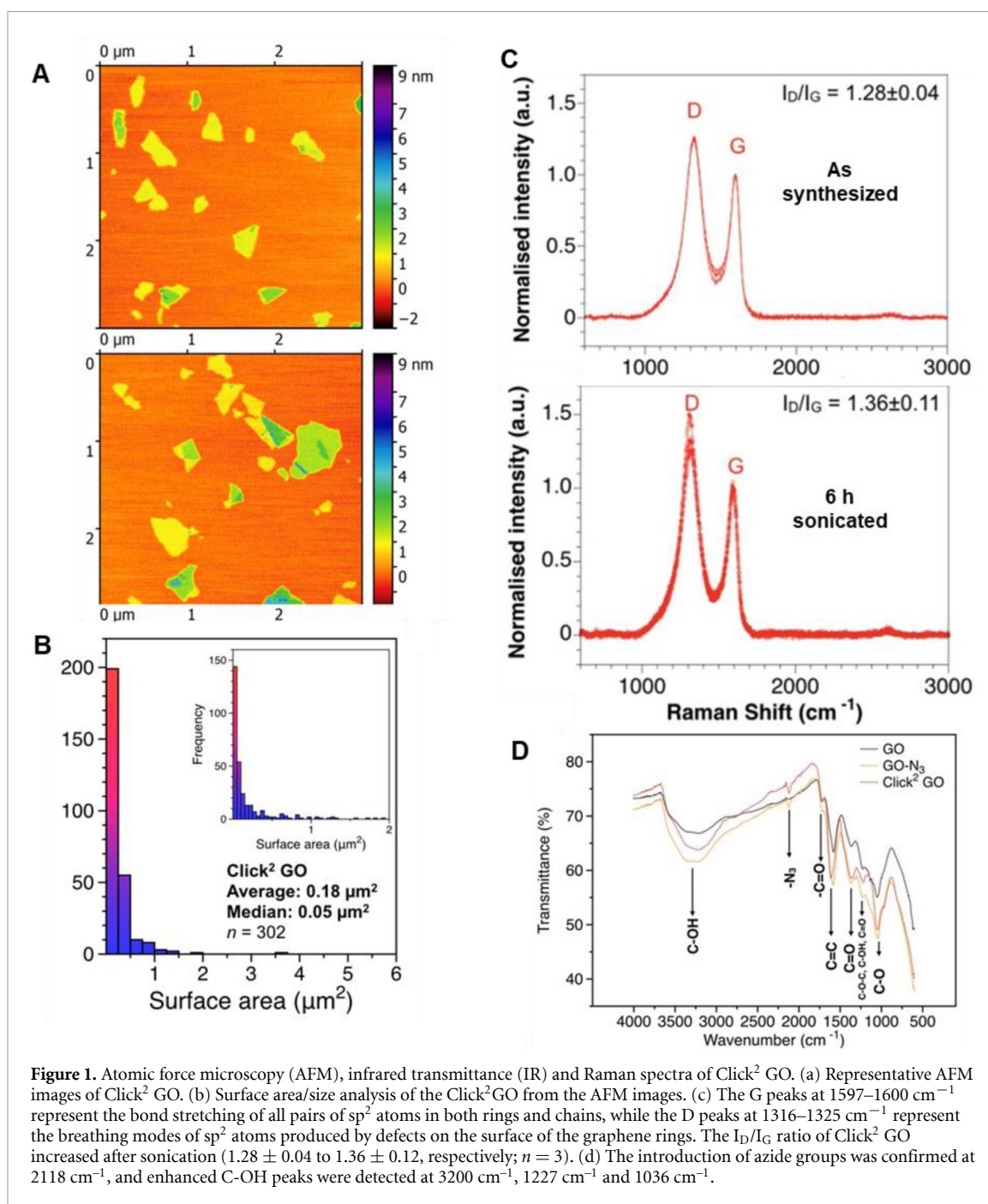
Since an effect on cell viability was primarily found for Click² GO, experiments tested whether Click² GO could affect the oxidative balance in cells by measuring the activity of the superoxide dismutase (SOD), an anti-oxidant enzyme that catalyses the dismutation of the superoxide anion (O_2^-) into H_2O_2 and O_2 . Similar to our previous observation with the cell viability assay, a concentration-dependent reduction in SOD activity (*i.e.* higher oxidative stress) was detected in G26, G7 and GL261 cells (figure 3). Unlike cell viability, however, the most pronounced changes were found in G7 (>4-fold reduction in SOD activity *vs* control) and G26 cells (>2-fold reduction in SOD activity *vs* control) exposed to 100 $\mu\text{g ml}^{-1}$ Click² GO for 24 h. Interestingly, prolonged incubation with Click² GO reversed this effect in G7 and G26 cells but not in GL261.

3.4. Double functionalised GO induces antiproliferative effects on GL261 cells

To clarify the mechanisms by which Click² GO compromises the viability of proliferating cells (G26, G7 and GL261), initial experiments assessed cell proliferation using the CellTrace™ kit. In this assay, a cell-permeant non-fluorescent molecule is converted to a fluorescent derivative by cellular esterase and retained by the cells. Cell division results in daughter cells receiving half of the fluorescent label of parent cells, *i.e.* fluorescence intensity is diluted with cell proliferation. In this regard, a small but significant increase in mean fluorescence intensity (indicative of reduced cell division) was only detected in non-stem cancer cells GL261 treated with 100 $\mu\text{g ml}^{-1}$ Click² GO for 72 h (~115% MFI, $p < 0.05$) (figure 4).

3.5. Double functionalised GO alters lipid and protein signatures of GL261 and GSCs, respectively

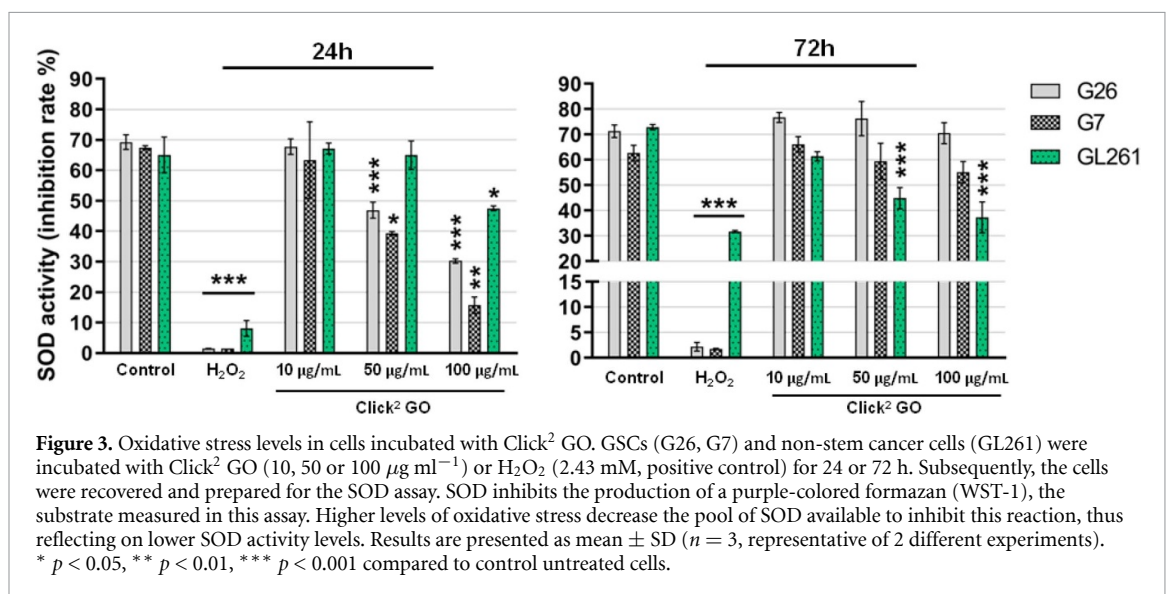
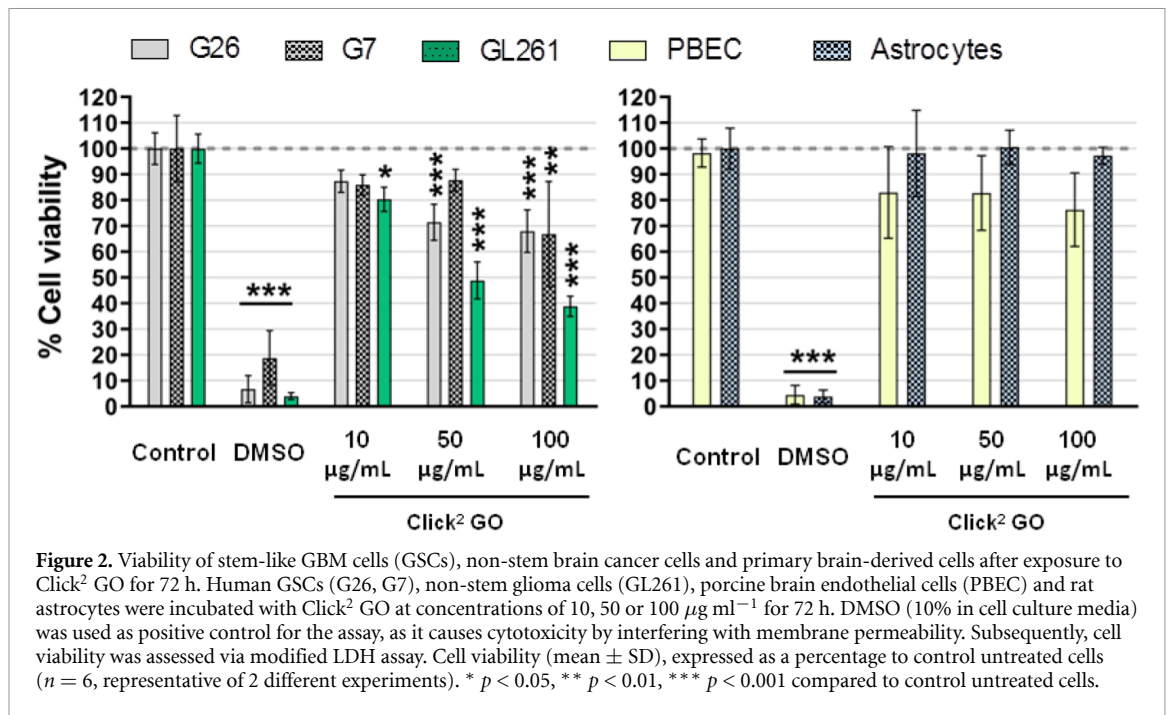
To further explore the Click² GO toxicities, we assessed biochemical changes in cell components after exposure to Click² GO by synchrotron radiation-based Fourier-transform infrared (SR-FTIR) spectromicroscopy. Differences in the resulting infrared spectra were analysed using principal component analysis (PCA). Analysis of the PCA score plots for the lipid region of the IR spectra (3100–2800 cm^{-1}) revealed significant separation in principal component 1 (PC-1) for GL261 exposed to 10 or 50 $\mu\text{g ml}^{-1}$ (figure 5) ($p < 0.05$). The corresponding loading plots (figure S4) confirmed that biochemical changes in this cell line correspond well with changes in the symmetric and asymmetric CH_2 vibrational modes



of the lipid molecules. The most pronounced separation in the protein region (1710–1470 cm⁻¹) was found in G26 cells, followed by G7 and GL261 cells when exposed to Click² GO at 10 and 50 μg ml⁻¹ (*p* < 0.05). The PCA loading plots show IR spectral changes in the Amide I and II regions due to biochemical changes caused by exposure to Click² GO (figure S4). Spectral changes in the protein region of GL261 could, nevertheless, be the result of the infrared absorption of Click² GO at 1616 cm⁻¹. These data suggest that toxicities observed in GL26 and G26 are linked to changes in lipid and proteins structures, respectively.

3.6. GL261 exhibits the highest association with Click² GO compared to other cells

Due to expected variability in the degree of uptake among the cell types studied and taking advantage of the strong D and G bands of Click² GO, Raman spectroscopy was used to assess association/interaction between Click² GO and the tested cells. Association/interaction between cells and Click² GO appeared to vary with cell line and concentration (figure 6(a), red signals). D-band intensities, normalized to the cell area, were quantified to compare the degree of cell association indirectly. A significant increase in intensity was found



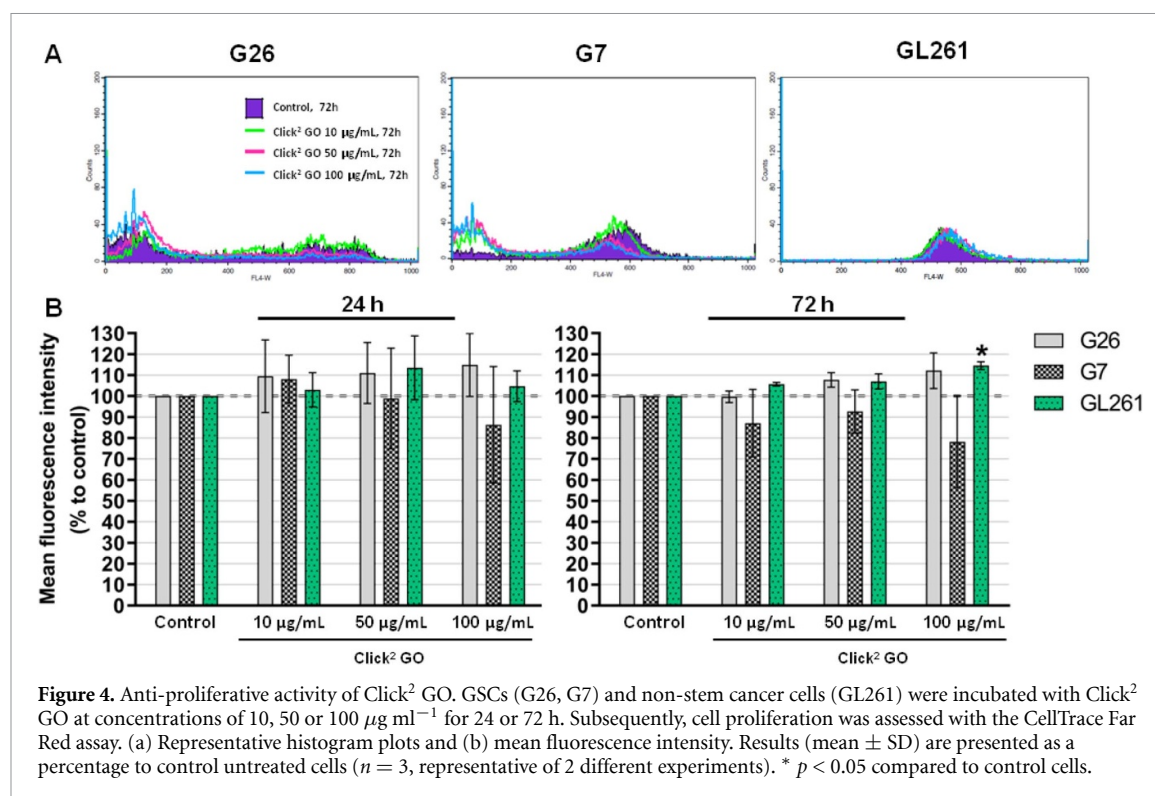
in GL261 cells, compared to the other tested cells (figure 6(b)). Decreased cell confluency (*i.e.* the number of cells per substrate area) was also detected in GL261 cells and, to a smaller extent, G26 cells incubated with 50 $\mu\text{g ml}^{-1}$ Click² GO (figure 6(c)). The results suggested that increased sensitivity of GL261 to Click² GO compared to other cells tested could be due to a combination of an enhanced association/interaction and type of biological responses exhibited by those cells.

4. Discussion

Driven by therapy-resistant quiescent stem-like cells (GSCs), GBM remains among the most lethal types of cancer. Despite the increased understanding of the

molecular alterations involved in therapy resistance [27] and promising experimental therapeutic options clinical outcomes have yet to improve, thus emphasizing the critical need for new therapeutic strategies that can deliver therapeutics widely in the adult brain.

Graphene-based nanomaterials have drawn significant interest for brain application as biomedical devices, due to their exceptional electrical and conductive properties, with studies showing potentiation of synaptic function or downregulation of neuronal signalling without affecting cell viability. Similarly, graphene nanocomposites have been tested as carriers for drug delivery and multimodal GBM therapy [28–32]. Chowdhury and co-workers developed DSPE-PEG-coated GO for delivery of lucanthonone to GBM, with results showing

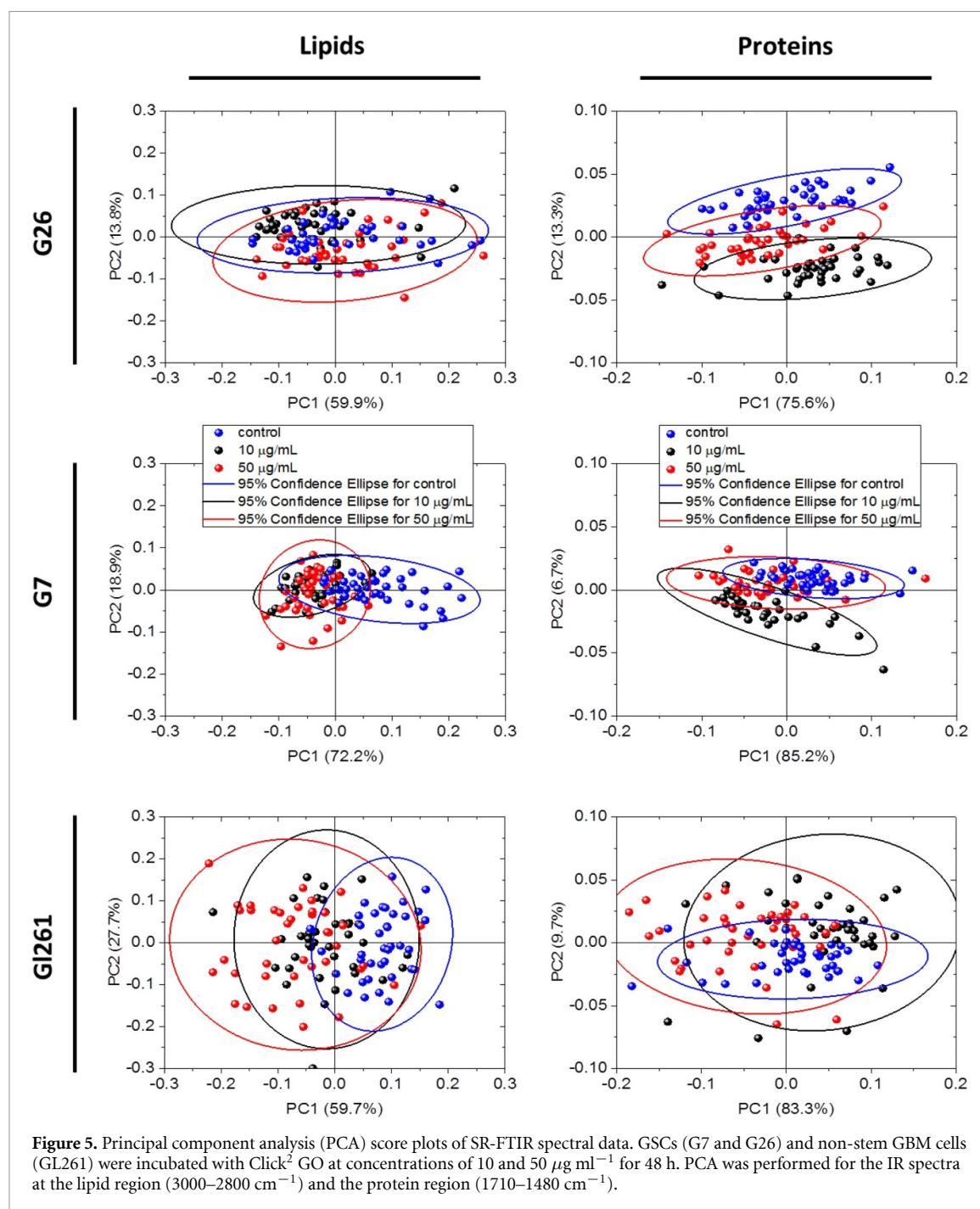


significant toxicity towards cultured U251 GBM cells and minimal toxicity to glial progenitor cells [28]. Song and colleagues constructed multifunctional GO-Fe₃O₄ nanocomposites, targeted to brain cancer via conjugation to lactoferrin, which showed good biocompatibility, large doxorubicin loading capacity and enhanced intracellular delivery efficiency and cytotoxicity [32]. Dong and colleagues developed a multifunctional drug delivery system, combining transferrin-conjugated PEGylated GO and doxorubicin, for simultaneous chemo- and photothermal therapy, with results from intravenously treated glioma-bearing rats showing enhanced tumour cell death and prolonged survival compared to single therapy [29]. There is a growing interest in utilizing GO-based nanocarriers for glioblastoma delivery. A systematic study on how these carriers interact with classic GBM cell lines and GSC and impact on their viability is, however lacking.

Cell uptake of graphene is known to be cell-specific and is dependent on particle size and surface chemistry [33]. Protein-coated small GO nanosheets (~ 0.42 µm diameter) were shown to enter mesenchymal progenitor cells primarily by clathrin-mediated endocytosis, whereas larger nanosheets (~ 0.86 µm diameter) were predominantly phagocytosed [34]. Chatterjee and colleagues have also shown that GO could be internalized by HepG2 cells, while the more hydrophobic reduced GO (rGO) is prone to adsorption onto the cell surface without internalization [35]. The size of Click² GO used in this study was modulated by sonication for 6 h to achieve flake size reduction. While AFM analysis confirmed that

Click² GO flakes were smaller than the precursor GO, a significant reduction in flake could not be found after sonication (compared to pre-sonication stocks), which suggests that the smaller size of Click² GO results from the functionalization reaction. The effect of sonication on Click² GO could also be determined by Raman spectroscopy. The observation of post-sonication increases in I_D/I_G ratio (a measure of the defects presents in the structure) for Click² GO could suggest that this process introduces surface defects in the nanomaterial.

With the development of graphene-based products for medical and biological application, a wide range of *in vitro* and *in vivo* studies have tested the effect of these nanomaterials in different biological systems [30, 36–42]. In this regard, graphene-based nanomaterials were found to induce toxicity in target cells via different cellular mechanisms, including loss of membrane integrity [39], apoptosis and cell cycle alterations [43], oxidative stress and mitochondria activation [38, 44], and immunotoxicity [45]. Graphene-mediated cytotoxicity was not only related to material concentration but especially to their physicochemical properties, such as surface area [46], layer number, [46] lateral dimensions [34], hydrophobicity and surface chemistry. Surface functionalization is essential for biomedical application as pristine graphene has poor water dispersibility. Chemical modification (via oxidation/amidation) or conjugation to biomedical-grade polymers (such as polyethylene glycol, poly(ϵ -caprolactone) or dextran) has shown to improve biocompatibility and decrease toxicity [41, 47]. Interestingly, while studying the

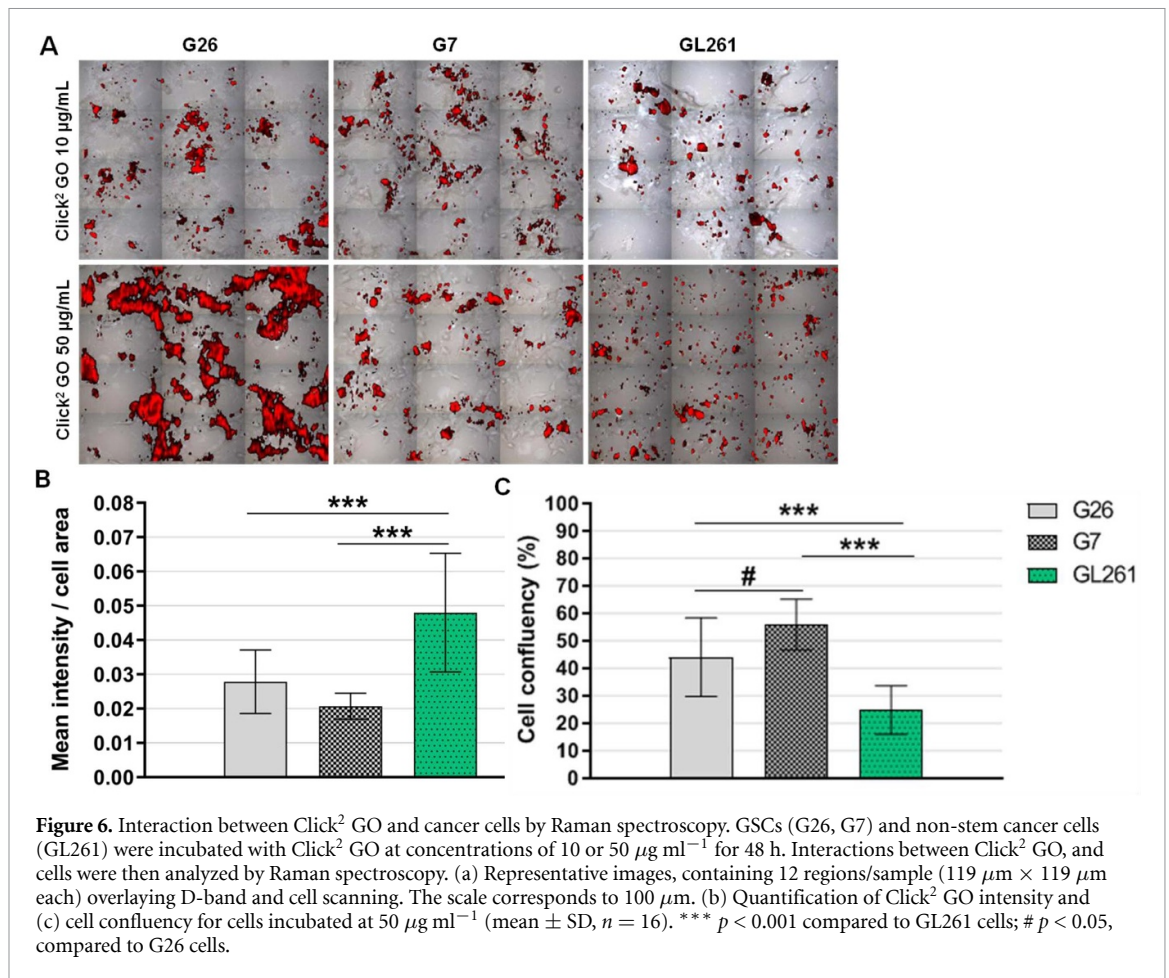


biocompatibility of GO and rGO towards cultured glioma cells, Jaworski and co-workers revealed uptake- and dose-dependent reduction in cell viability and proliferation, this effect was being more pronounced for rGO [30].

In our study, a stronger effect on cell viability was found for Click² GO on the non-stem glioma cell line GL261 followed by moderate effects on GSCs (G26) then no effect on the non-proliferating cells. GSCs culture media, for example, is serum-free (FCS is replaced by 0.011% BSA); we, therefore, anticipated higher toxicity for GSCs than serum grew cell lines (media containing 10% FCS). However, this was not the case. This suggests

that differences in association/interaction and toxicity profiles are related to intrinsic variability how the different cells respond to GO derivatives—both association/interaction and intra-cellular responses.

GL261 (most positive for Click² GO association/interaction) revealed small changes in cell proliferation for the highest tested concentration (100 $\mu\text{g ml}^{-1}$). More importantly, oxidative stress failed to return to normal levels at 72 h post-incubation. Moreover, those changes were accompanied by alterations in the biochemical signature of lipids. Interestingly, while a considerable increase in cell oxidative stress, reflected on the decrease in SOD



activity, could be detected in GSCs (namely G26), those returned to normal levels within 72 h. Since no alterations in the biochemical signature of lipids were found in GSCs, it could be hypothesised that the failure of GL261 cells to return oxidative stress to normal levels could be due, among others, to compromised membrane structures (reflected in alterations of the lipid profile). GSCs cells, however, showed significant changes in the biochemical signature of proteins (G26 > G7) suggesting that the effects detected at the cellular level could be caused by the interaction of Click² GO with these building blocks.

Findings in our study on interactions between GOs and GSCs differ from those reported by Fiorillo *et al*, which demonstrated GO treatment inhibited several stem cell-associated signal transduction pathways, e.g. WNT, Notch and STAT1/3, which affected tumour-sphere formation and induction of differentiation [48]; however, GO-related alterations in oxidative stress status and mitochondrial function could not be detected. An explanation could be that cancer stem cells were grown in suspension (as neurospheres) [48] in comparison to an adherent culture used in our study. The latter method has been previously validated and shown to provide a more uniform environment that suppresses spontaneous differentiation without the loss of stemness potential [4, 5, 19, 21]. Our results are, however, in line with

several other reports which have shown that GO is not toxic to normal stem cells and could be used as a growth substrate and to induce their differentiation into different lineages [49, 50].

5. Conclusions

Our results confirmed selective toxicity of Click² GO to highly proliferative GBM cell lines and patient GSCs, and minimal toxicity to primary brain astrocytes and endothelial cells. We conclude that a novel class of GBM-targeting graphene-based nanocarriers could be useful delivery vehicles for GBM therapeutics.

Acknowledgments

The authors would like to thank Houmam Kafa (King's College London) for the training and assistance with the isolation of PBEC cells and astrocytes. Kuo-Ching Mei is supported by Graduate School International Research Award. Pedro M. Costa is a Sir Henry Wellcome Post-doctoral fellow (WT103913).

Disclosure of interest

The authors report no conflict of interest.

ORCID iDs

Pedro M Costa  <https://orcid.org/0000-0003-0196-8649>

Kuo-Ching Mei  <https://orcid.org/0000-0001-6045-2154>

Martin Kreuzer  <https://orcid.org/0000-0002-7305-5016>

Frederic Festy  <https://orcid.org/0000-0002-3939-8437>

Steven M Pollard  <https://orcid.org/0000-0001-6428-0492>

Khuloud T Al-Jamal  <https://orcid.org/0000-0001-5165-2699>

References

- [1] Stupp R et al 2009 *Lancet Oncol.* **10** 459–66
- [2] Galli R, Binda E, Orfanelli U, Cipelletti B, Gritti A, De Vitis S, Fiocco R, Foroni C, Dimeco F and Vescovi A 2004 *Cancer Res.* **64** 7011–21
- [3] Singh S K, Hawkins C, Clarke I D, Squire J A, Bayani J, Hide T, Henkelman R M, Cusimano M D and Dirks P B 2004 *Nature* **432** 396–401
- [4] Pollard S M et al 2009 *Cell Stem Cell* **4** 568–80
- [5] Lathia J D et al 2012 *Ann. Neurol.* **72** 766–78
- [6] Lee J et al 2006 *Cancer Cell* **9** 391–403
- [7] Novoselov K S, Geim A K, Morozov S V, Jiang D, Zhang Y, Dubonos S V, Grigorieva I V and Firsov A A 2004 *Science* **306** 666–9
- [8] Sun X, Liu Z, Welsher K, Robinson J T, Goodwin A, Zaric S and Dai H 2008 *Nano Res.* **1** 203–12
- [9] Bao H, Pan Y, Ping Y, Sahoo N G, Wu T, Li L, Li J and Gan L H 2011 *Small* **7** 1569–78
- [10] Kim H, Namgung R, Singha K, Oh I-K and Kim W J 2011 *Bioconjug. Chem.* **22** 2558–67
- [11] Robinson J T, Tabakman S M, Liang Y, Wang H, Sanchez Casalongue H, Vinh D and Dai H 2011 *J. Am. Chem. Soc.* **133** 6825–31
- [12] Li J-L, Tang B, Yuan B, Sun L and Wang X-G 2013 *Biomaterials* **34** 9519–34
- [13] Lallana E, Sousa-Herves A, Fernandez-Trillo F, Rigueria R and Fernandez-Megia E 2012 *Pharm. Res.* **29** 1–34
- [14] Mei K-C et al 2018 *Adv. Mater.* **30** 1802732
- [15] Mei K-C, Guo Y, Bai J, Costa P M, Kafa H, Protti A, Hider R C and Al-Jamal K T 2015 *ACS Appl. Mater. Interfaces* **7** 14176–81
- [16] Mei K-C, Rubio N, Costa P M, Kafa H, Abbate V, Festy F, Bansal S S, Hider R C and Al-Jamal K T 2015 *Chem. Commun.* **51** 14981–4
- [17] Rubio N et al 2015 *ACS Appl. Mater. Interfaces* **7** 18920–3
- [18] Rubio N et al 2014 *Langmuir* **30** 14999–5008
- [19] Danovi D et al 2013 *PLoS ONE* **8** e77053
- [20] Bulstrode H et al 2017 *Genes Dev.* **31** 757–73
- [21] Stricker S H et al 2013 *Genes Dev.* **27** 654–69
- [22] Carén H et al 2015 *Stem Cell Rep.* **5** 829–42
- [23] Abbott N J, Dolman D E M, Drndarski S and Fredriksson S M 2012 An improved *In Vitro* blood–brain barrier model: rat brain endothelial cells co-cultured with astrocytes *Astrocytes: Methods and Protocols* ed R Milner (NJ: Humana Press: Totowa) pp 415–30
- [24] Rubin L L, Hall D E, Porter S, Barbu K, Cannon C, Horner H C, Janatpour M, Liaw C W, Manning K and Morales J 1991 *J. Cell Biol.* **115** 1725–35
- [25] Varotsis C and Vamvouka M 1999 *J. Phys. Chem. B* **103** 3942–6
- [26] Ali-Boucetta H, Al-Jamal K T and Kostarelos K 2011 Cytotoxic assessment of carbon nanotube interaction with cell cultures *Biomedical Nanotechnology: Methods and Protocols* ed S J Hurst (Totowa, NJ: Humana Press) pp 299–312
- [27] Auffinger B, Spencer D, Pytel P, Ahmed A U and Lesniak M S 2015 *Expert Rev. Neurother.* **15** 741–52
- [28] Chowdhury S M, Surhland C, Sanchez Z, Chaudhary P, Suresh Kumar M A, Lee S, Peña L A, Waring M, Sitharaman B and Naidu M 2015 *Nanomed. Nanotechnol. Biol. Med.* **11** 109–18
- [29] Dong H, Jin M, Liu Z, Xiong H, Qiu X, Zhang W and Guo Z 2016 *Lasers Med. Sci.* **31** 1123–31
- [30] Jaworski S, Sawosz E, Kutwin M, Wierzbicki M, Hinzmann M, Grodzik M, Winnicka A, Lipinska L, Wlodyga K and Chwalibog A 2015 *Int. J. Nanomed.* **10** 1585–96
- [31] Sawosz E et al 2015 *Int. J. Mol. Sci.* **16** 25214–33
- [32] Song -M-M, Xu H-L, Liang J-X, Xiang -H-H, Liu R and Shen Y-X 2017 *Mater. Sci. Eng. C* **77** 904–11
- [33] Zhang B, Wei P, Zhou Z and Wei T 2016 *Adv. Drug Deliv. Rev.* **105** 145–62
- [34] Ma J, Liu R, Wang X, Liu Q, Chen Y, Valle R P, Zuo Y Y, Xia T and Liu S 2015 *ACS Nano* **9** 10498–515
- [35] Chatterjee N, Eom H-J and Choi J 2014 *Biomaterials* **35** 1109–27
- [36] Akhavan O and Ghaderi E 2010 *ACS Nano* **4** 5731–6
- [37] Akhavan O, Ghaderi E and Akhavan A 2012 *Biomaterials* **33** 8017–25
- [38] Chen M, Yin J, Liang Y, Yuan S, Wang F, Song M and Wang H 2016 *Aquat. Toxicol.* **174** 54–60
- [39] Liao K-H, Lin Y-S, Macosko C W and Haynes C L 2011 *ACS Appl. Mater. Interfaces* **3** 2607–15
- [40] Yang K, Gong H, Shi X, Wan J, Zhang Y and Liu Z 2013 *Biomaterials* **34** 2787–95
- [41] Yang K, Wan J, Zhang S, Zhang Y, Lee S-T and Liu Z 2011 *ACS Nano* **5** 516–22
- [42] Zhang W et al 2012 *Adv. Mater.* **24** 5391–7
- [43] Kang Y, Liu J, Wu J, Yin Q, Liang H, Chen A and Shao L 2017 *Int. J. Nanomed.* **12** 5501–10
- [44] Jarosz A, Skoda M, Dudek I and Szukiewicz D 2016 *Oxid. Med. Cell. Longevity* **2016** 5851035
- [45] Cho Y C, Pak P J, Joo Y H, Lee H-S and Chung N 2016 *Sci. Rep.* **6** 38884
- [46] Sanchez V C, Jachak A, Hurt R H and Kane A B 2012 *Chem. Res. Toxicol.* **25** 15–34
- [47] Zhang S, Yang K, Feng L and Liu Z 2011 *Carbon* **49** 4040–9
- [48] Fiorillo M, Verre A F, Iliut M, Peiris-Pagés M, Ozsvári B, Gandara R, Cappello A R, Sotgia F, Vijayaraghavan A and Lisanti M P 2015 *Oncotarget* **6** 3553–62
- [49] Garcia-Alegria E, Iliut M, Stefanska M, Silva C, Heeg S, Kimber S J, Kouskoff V, Lacaud G, Vijayaraghavan A and Batta K 2016 *Sci. Rep.* **6** 25917
- [50] Yang D, Li T, Xu M, Gao F, Yang J, Yang Z and Le W 2014 *Nanomedicine* **9** 2445–55